We are IntechOpen, the world's leading publisher of Open Access books Built by scientists, for scientists

4,800
Open access books available

122,000
International authors and editors

135M
Downloads

Our authors are among the

154
Countries delivered to

TOP 1%
most cited scientists

12.2%
Contributors from top 500 universities

CLARIVATE ANALYTICS BOOK CITATION INDEX INDEXED

WEB OF SCIENCE™

Selection of our books indexed in the Book Citation Index in Web of Science™ Core Collection (BKCI)

Interested in publishing with us?
Contact book.department@intechopen.com

Numbers displayed above are based on latest data collected.
For more information visit www.intechopen.com

13

Quantum Computing and Optimal Control Theory

Kenji Mishima
Research Center for Advanced Science and Technology,
The University of Tokyo, Komaba, Meguro-ku, Tokyo
Japan

1. Introduction

In recent years, quantum computing and quantum information science have become one of the most important and attractive research areas in a variety of disciplines, e. g., mathematics, information science, physics, chemistry, etc[1]. These new kinds of technologies are predicted to be much more advantageous compared with the classical computers and classical information science and the benefit obtained by these technologies is assumed to be beyond measure in our every-day life. For instance, quantum computers are predicted to be able to solve mathematical problems that today's fastest computers could not solve in years. In particular, entanglement or entangled state plays a key role for quantum computing and quantum information processing. For example, arbitrary quantum states of two-level system can be teleported through classical communication with the help of maximally entangled Bell state from one place to other macroscopic distant places (quantum teleportation)[2], which has no counterpart in classical mechanics. As opposed to the quantum teleportation, classical information can be teleported by using the maximally entangled Bell state (superdense coding)[3]. Needless to say, entanglement is also an essential ingredient in quantum computing[1].

At present, theoretical investigations of the mechanism of quantum computing and quantum information science have become mature although some of the important theoretical problems, e. g., definition of entanglement degree of multipartite systems, have not yet been solved and are still controversial. Yet, one can say that we are now reaching a stage of experimental realizations of quantum computing and quantum information processing proposed and investigated theoretically and numerically. To apply quantum computing and quantum information processing to realistic quantum systems, a number of microscopic quantum systems have been proposed. Just to mention a few, cavity quantum electrodynamics (cavity QED)[4], trapped ions[5 - 7], neutral atoms trapped in optical lattices[8], nuclear magnetic resonance (NMR)[9, 10], superconducting circuits[11], silicon-based nuclear spin[12], diamond-based quantum computer[13, 14] are some of the promising candidates of quantum computing devices.

However, investigation of utilization of molecular internal degrees of freedom for quantum computing and quantum information science, in particular, electronic, vibrational, and rotational degrees of freedom, is still in its infancy. Although molecules are also quantum systems, very few chemists have yet examined how to use molecular internal degrees of

freedom for quantum computing and quantum information science from the chemical viewpoint. The pioneering numerical investigation of usage of molecular vibrational states for constructing elementary quantum gates was reported by de Vivie-Riedle and coworkers at the beginning of this century[15]. Later on, they have stick to pursuing "molecular vibrational" quantum computing in a number of papers[16 - 21]. Soon after their works, some of the other research groups have extended their works and have proposed new ideas of quantum computing and quantum information science[22 - 30]. The purpose of many of these works is to numerically construct elementary gate pulses using optimal control theory (OCT)[31]. Instead of using tailored laser pulses, Teranishi and coworkers have developed a quantum computation scheme to process arbitrary quantum gate operations by using the free propagation of the wavepacket of I_2 molecule[32]. Anyway, OCT that has originally stemmed from the necessity of control of chemical reactions has become one of the main procedures for constructing the quantum gates.

Although the "vibrational" quantum computers are the mainstream for the investigations of molecular quantum computing, two-qubit system consisting of one vibrational and one rotational modes of molecules has also been investigated by several researchers[33, 34]. In[33], single- and two- qubit operations, e. g., NOT and CNOT gates, within rotational and vibrational states of a diatomic molecule using strong-field molecular alignment is proposed. Numerical calculations of IR quantum gate pulses for $^{12}C^{16}O$ molecule using a genetic algorithm instead of employing OCT have been investigated by Momose and coworkers[34].

Another possibility is to use *inter*molecular states instead of the *intra*molecular states mentioned above. In[35], one of the methods of realizing quantum phase gate and generation of entanglement rotational modes of two polar molecules coupled by dipole-dipole interaction has been proposed. Unlike their research, we have numerically constructed several universal gates and applied them to the Deutsch-Jozsa algorithm[36].

On the other hand, attempts of experimental realizations of quantum computers using molecular internal degrees of freedom have also begun to be done in recent years. For example, Vala and coworkers experimentally demonstrated the Deutsch-Jozsa algorithm for three-qubit functions by utilizing pure coherent superposition states of Li_2 rovibrational eigenstates[37]. Rovibrational wave-packet manipulation using phase- and amplitude- modulated midinfrared femtosecond laser pulses for $^{12}C^{16}O$ and $^{14}N^{16}O$ molecules have been investigated experimentally and numerically by Momose and coworkers for the purpose of applying their techniques to quantum computing[38]. Ohmori and coworkers experimentally demonstrated coherent control of wavepacket interference, wavepacket interferometry, using vibraiontal wavepackets of I_2 molecule with the aim of retrieving quantum information such as amplitudes and phases of eigenfunctions involved in the wavepacket[39 - 43].

This present situation mentioned above implies that the research of quantum computing using molecular internal degrees of freedom is gradually attracting many physical chemists and chemical physicists in quite recent years.

Interesting aspects of molecules compared with physical systems such as atoms, photons, electron spins, nuclear spins, etc. are that they possess a variety of quantum mechanical internal degrees of freedom. If we restrict ourselves only to two-qubit systems, several kinds of combinations of modes can be considered. The two-qubit combination studied most frequently is vibrational-vibrational qubit combination as mentioned above. Since the investigation of molecular quantum computers is still immature, we predict that there will

be a number of unsolved problems up to now and recommend chemists to investigate molecular quantum computing in more detail in the future although many of the chemists including us have already contributed to the improvement of the molecular quantum computers. For example, we may expect that scalable quantum computing using many internal degrees of freedom will be realized in the future.

The present chapter is organized as follows. In Section 2, we first introduce some of the basic concepts of quantum computers for the convenience of those who are not familiar with quantum computers. One of the most important quantum algorithms, Deutsch-Jozsa algorithm, is also explained shortly. Then, for this chapter to be self-contained, OCT will briefly be reviewed because molecular quantum computing strongly relies on OCT as mentioned above. In Section 3, our development of free-time and fixed end-point optimal control theories (FRFP-OCTs) without and with dissipation is presented and the theory and the algorithm are applied to entanglement generation and maintenance. One will find that the FRFP-OCT is more convenient and advantageous than the conventional fixed end-point optimal control theory (FIFP-OCT). Finally, Section 4 is devoted to concluding remarks.

2. Quantum algorithms

2.1 Quantum gates

Quantum gates are the counterparts of logic gates of classical computer circuits. The definition of operations of the classical single bit logic gates is given by truth table. For example, the operation of NOT gate is to flip the bits: $0 \to 1$ and $1 \to 0$.

In what follows, we list some of the most important quantum gates that are usually used in quantum circuits:

Hadamard gate: $H_{dm} = \frac{1}{\sqrt{2}}\begin{bmatrix} 1 & 1 \\ 1 & -1 \end{bmatrix}$ for single-qubit gate,

NOT gate: $NOT = \begin{bmatrix} 0 & 1 \\ 1 & 0 \end{bmatrix}$ for single-qubit gate,

CNOT (controlled-not) gate: $CNOT = \begin{bmatrix} 1 & 0 & 0 & 0 \\ 0 & 1 & 0 & 0 \\ 0 & 0 & 0 & 1 \\ 0 & 0 & 1 & 0 \end{bmatrix}$ for two-qubit gate,

ID gate: $ID = \begin{bmatrix} 1 & 0 \\ 0 & 1 \end{bmatrix}$ for single-qubit gate,

Z gate: $Z = \begin{bmatrix} 1 & 0 \\ 0 & -1 \end{bmatrix}$ for single-qubit gate,

$\pi/8$ gate: $T = \begin{bmatrix} 1 & 0 \\ 0 & \exp(i\pi/4) \end{bmatrix}$ for single-qubit gate,

phase gate: $S = \begin{bmatrix} 1 & 0 \\ 0 & i \end{bmatrix}$ for single-qubit gate,

Toffoli gate: $U_T = \begin{bmatrix} 1 & 0 & 0 & 0 & 0 & 0 & 0 & 0 \\ 0 & 1 & 0 & 0 & 0 & 0 & 0 & 0 \\ 0 & 0 & 1 & 0 & 0 & 0 & 0 & 0 \\ 0 & 0 & 0 & 1 & 0 & 0 & 0 & 0 \\ 0 & 0 & 0 & 0 & 1 & 0 & 0 & 0 \\ 0 & 0 & 0 & 0 & 0 & 1 & 0 & 0 \\ 0 & 0 & 0 & 0 & 0 & 0 & 0 & i \\ 0 & 0 & 0 & 0 & 0 & 0 & -i & 0 \end{bmatrix}$ for three-qubit gate.

For processing the quantum computation, the two-level unitary gates such as shown above must be universal[48]. Here, the term "universal" means that one can implement an arbitrary two-level unitary transformation on the space of arbitrary numbers of qubits. For example, using the Gray codes, it has been proven that single qubit and CNOT gates are universal[1]. It should be emphasized that the gobal unitary transformations such as CNOT gate cannot be reduced to the direct product of two single-qubit gates. Therefore, if the total Hamiltonian can be reduced to the product of two single-qubit unitary transformations, it is impossible to perform universal quantum computation and quantum information processing.

2.2 Deutsch-Jozsa algorithm

So far, several quantum algorithms have been proposed which outperform the corresponding classical algorithms. These include the Grover's algorithm, Shor's algorithm, the quantum Fourier transform, the Deutsch-Jozsa algorithm, etc.[1]. For example, the Shor's algrorithm is a quantum algorithm for integer factorization[51]. On a quantum computer, to factor an integer N, Shor's algorithm takes polynomial time in log$N$, specifically O((log$N$)^3), demonstrating that integer factorization is in the complexity class BQP. This is exponentially faster than the best-known classical factoring algorithm.

For instance, the flowchart of the two-state Deutsch-Jozsa algorithm is shown in Fig. 1. In short, the story of the Deutsch-Jozsa algorithm is as follows. Let us assume two persons, Alice and Bob. Alice holds the so-called query register while Bob holds the so-called answer register. First, they come close together and they make some promises before they go far apart from each other. When they are close together, Alice promises to send the number 0 or 1 to Bob and he promises to calculate some function f and to send her the answer 0 or 1. At this time, Bob promises to use two kinds of functions f. That is, he sends her the same number for all the numbers that he obtains from her (constant function) or he sends 0 for half of the numbers that he obtains from her and 1 for the remaining half (balanced function). After that, they go far apart from each other. The purpose of this algorithm is that Alice must clarify whether the function f that Bob applies is constant or balanced, which is contained in the oracle denoted by U_f. It is known that classically the algorithm scales as $O(2^n)$, while quantum-mechanically it scales as $O(n)$, where n is the number of qubit registers that Alice holds. This demonstrates the significant speedup of quantum parallelism compared with classical algorithms, in particular, when n is very large. In other words, the advantage of quantum parallelism is obtained when the quantum circuit becomes very large.

In the flowchart of Fig. 1, the initial state of the whole Hilbert space is $|00\rangle$. First, Bob applies the NOT gate and the transition $|00\rangle \rightarrow |01\rangle$ occurs. Bob then applies the Hadamard

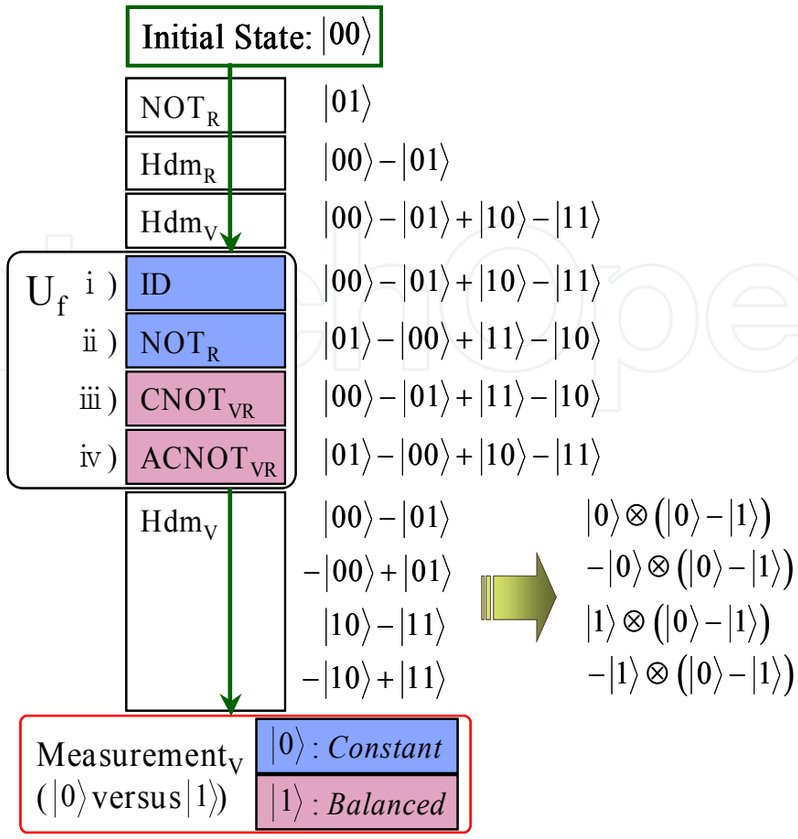

Fig. 1. The two-state Deutsch-Jozsa algorithm

gate Hdm_R and Alice the Hadamard gate Hdm_V. At this moment, the state of the whole system becomes $|00\rangle-|01\rangle+|10\rangle-|11\rangle$. To this quantum superposition state, the unitary transformation, the so-called oracle,

$$U_f : |x,y\rangle \rightarrow |x,y \oplus f(x)\rangle, \tag{1}$$

is applied. Here, $\oplus$ denotes addition modulo 2. The rule of Eq. (1) must be applied for all four possible definitions of f. According to the four definitions, U_f is defined by the four operations (i) ~ (iv) in Fig. 1. Alice then applies the Hadamard transformation Hdm_V. If she recognizes that she obtains the state $\pm|0\rangle$ by her own measurement, f is constant, while f is balanced if she obtains the state $\pm|1\rangle$. These states can be distinguished by measuring her own qubit as shown in Fig. 1.

In Fig. 1, the subscripts of the first and the second entries for elementary quantum gates refer to control bit and target bit, respectively. Here, the abbreviations, V, and R, stand for vibrational and rotational states, respectively.

2.3 Optimal control theory (OCT): General theory and application to molecular quantum computers

As already mentioned in Section 1, to process quantum computing, it is necessary to tailor elementary gate laser pulses appropriately. This particularly holds for molecules. This is because unlike spins molecular modes of internal degrees of freedom are essentially

"qudits", not "qubits." In this section, we will briefly review conventional OCT and multi-target OCT (MTOCT). For more details, we recommend the readers to refer to [52, 53].

If the purpose is just to drive one specific wave function $\psi_i(t)$ to the desired wave function $\Phi(T)$ at the fixed time $t = T$, the objective functional to be maximized is given by[52]

$$J = \left|\langle\psi_i(T)|\Phi(T)\rangle\right|^2 - \alpha_0\int_0^T [E(t)]^2\,dt \\ -2\,\mathrm{Re}\left[\langle\psi_i(T)|\Phi(T)\rangle \times \int_0^T \langle\psi_f(t)|\frac{\partial}{\partial t} + i[H_0 + V - \mu E(t)]|\psi_i(t)\rangle\,dt\right], \tag{2}$$

where H_0 is the zero-th order Hamiltoinian, V is the potential energy, μ is the transition dipole moment, $E(t)$ is the laser pulse to be optimized, and T is the fixed final time of the laser pulse. The second term restricts the laser intensity, where α_0 is usually called the penalty factor. $|\psi_f(t)\rangle$ is the Lagrange multiplier for $|\psi_i(t)\rangle$.

To incorporate the effect of slow turn-on and turn-off of the laser pulses adequate for practical experimental tailoring, the penalty factor in Eq. (2) is replaced by[53]

$$-\alpha_0\int_0^T \frac{[E(t)]^2}{s(t)}\,dt\,, \tag{3}$$

where

$$s(t) = \sin^2(\pi t / T)\,. \tag{4}$$

In this case, the optimized external field is expressed as

$$E(t) = -\frac{s(t)}{\alpha_0}\mathrm{Im}\left\{\langle\psi_i(t)|\psi_f(t)\rangle\langle\psi_f(t)|\mu|\psi_i(t)\rangle\right\}. \tag{5}$$

Although the above formalisms may be applicable to tailoring the gate laser pulses for any quantum control problems, they are not appropriate for tailoring *general-purpose* global gate pulses that are required for quantum computing. In other words, the given gate pulse has to process the given quantum gate for any input states and the corresponding output states. In this case, one of the best choices is to resort to multi-target optimal control theory (MTOCT)[54]. For MTOCT, the objective functional to be maximized is given by

$$J_{MTOCT} = \sum_{k=1}^{z}\left\{\left|\langle\psi_{ik}(T)|\Phi_{fk}(T)\rangle\right|^2 - \alpha_0\int_0^T \frac{[E(t)]^2}{s(t)}\,dt \right. \\ \left. -2\,\mathrm{Re}\left\{\langle\psi_{ik}(T)|\Phi_{fk}(T)\rangle \times \int_0^T \langle\psi_{fk}(t)|\frac{\partial}{\partial t} + i[H_0 + V - \mu E(t)]|\psi_{ik}(t)\rangle\,dt\right\}\right\}, \tag{6}$$

where z is the number of control targets, k denotes the number of targets ranging from 1 to z, $|\Phi_{fk}(T)\rangle$ is the k-th target at time $t = T$, $|\psi_{ik}(t)\rangle$ is the wavefunction of the system of the k-th target, and $|\psi_{fk}(t)\rangle$ is the Lagrange multiplier for $|\psi_{ik}(t)\rangle$. In this case, the optimal external field reads

$$E(t) = -\frac{zs(t)}{\alpha_0}\sum_{k=1}^{z}\mathrm{Im}\left\{\left\langle\psi_{ik}(t)\middle|\psi_{fk}(t)\right\rangle\left\langle\psi_{fk}(t)\middle|\mu\middle|\psi_{ik}(t)\right\rangle\right\}. \tag{7}$$

The number of the control targets z has to be chosen as follows. Recently, de Vivie-Riedle and coworkers[17] proposed a method for phase-correct and basis-set-independent quantum gates in order to perform the correct universal quantum computing. As far as we know, their work is the first one where the phase correction was taken into account adequately. The requirement of the phase-correct quantum gate is that, for example, the NOT operation for the superposition state,

$$|00\rangle + |01\rangle + |10\rangle + |11\rangle \rightarrow \left(|01\rangle + |00\rangle + |11\rangle + |10\rangle\right)e^{i\varphi_5}, \tag{8}$$

must be optimized in addition to the following four conventional pure basis state optimizations,

$$|00\rangle \rightarrow |01\rangle e^{i\varphi_1},$$

$$|01\rangle \rightarrow |00\rangle e^{i\varphi_2},$$

$$|10\rangle \rightarrow |11\rangle e^{i\varphi_3},$$

$$|11\rangle \rightarrow |10\rangle e^{i\varphi_4}. \tag{9}$$

If we do not impose the requirement of Eq. (8), the superposition state will evolve as:

$$|00\rangle + |01\rangle + |10\rangle + |11\rangle \rightarrow |01\rangle e^{i\varphi_1} + |00\rangle e^{i\varphi_2} + |11\rangle e^{i\varphi_3} + |10\rangle e^{i\varphi_4}, \tag{10}$$

which is not the correct NOT operation, because in general $\varphi_1 \neq \varphi_2 \neq \varphi_3 \neq \varphi_4$. Likewise, we must impose additional constraints for the other quantum gates we have in mind. As de Vivie-Riedle and coworkers pointed out[17], the phase correction of quantum gates is one of the key issues for the implementation of quantum algorithms. Therefore, for two-qubit systems, z has to be more than 4.

There are two methods to measure the gate fidelities: the average transition probability given by

$$\overline{P} = \frac{1}{z}\sum_{k=1}^{z}\left|\left\langle\psi_{ik}(T)\middle|\Phi_{fk}(T)\right\rangle\right|^2, \tag{11}$$

and the fidelity expressed as

$$F = \frac{1}{z^2}\left|\sum_{k=1}^{z}\left\langle\psi_{ik}(T)\middle|\Phi_{fk}(T)\right\rangle\right|^2. \tag{12}$$

The average transition probability cannot take into account the phase relation between $\psi_{ik}(T)$ and $\Phi_{fk}(T)$, while the fidelity can. If one uses the average transition probability, the phase correction cannot be determined, while the fidelity is useful for clarifying the phase

correction. Therefore, we must define the laser pulses that have the largest fidelity as the optimal gate pulses.

3. Free-time and fixed end-point optimal control theory (FRFP-OCT)

In a series of our publications[55, 56], we have found that the entanglement generation in general quantum systems crucially rely on the strength of entangling interactions among distinct quantum systems. We have stressed that if the entangling interactions are strong, the maximally entangled state can be created in a short time. This in turn implies that if the strength of the entangling interactions is weak, long laser fields are necessary for creating the maximally entangled states. Approximately, the time duration of the laser pulses by which the maximally entangled states can be created is inversely proportional to the strength of the entangling interaction. Therefore, it can easily be recognized that we need a new OCT that works well even if we do not know the necessary time duration of the laser pulses to create the maximally entangled state efficiently because the actual entangling interactions are usually much more complicated in molecular systems. If this is the case, the necessary OCT will become *free-time* and fixed end-point optimal control theory (FRFP-OCT) since the optimal temporal duration of the laser pulses is not known exactly in advance. Currently, OCT in quantum systems proposed so far has been limited to the *fixed-time* and fixed end-point optimal control theory (FIFP-OCT)[57]. Consequently, we have constructed one of the versions of FRFP-OCTs that can optimize the objective functional and the temporal duration of the laser pulses simultaneously[58, 59]. One of the advantages of our theory is that one does not need to try various final fixed times to achieve the best control of quantum dynamics. To demonstrate the utility of our theory it has been applied to the optimization of laser pulses that can create maximally entangled states efficiently, but it may also be applied to various physical and chemical quantum control problems.

On the other hand, realistic quantum systems that we observe experimentally and calculate theoretically are always interacting with surrounding environment by way of entangling interactions. If the whole quantum system is the sum of the system of our interest and the huge surrounding environment, the quantum state is maintained in pure state (no decoherence). However, the surrounding environment is traced out and our attention is paid only to our small quantum system, our system becomes mixed state (decoherence). This can be easily verified by using, e. g., the von-Neumann entropy used to measure entanglement degree of the pure state of composite systems. In many quantum control problems, the decoherence is unfavorable and should be suppressed.

Quantum computing and quantum information science are also not exceptions. It was pointed out that the decoherence might become one of the crucial obstacles for quantum computers and entanglement generation and manipulation because quantum information processing must be performed in pure states in most cases[60, 61]. Therefore, to achieve accurate quantum computing and quantum information processing in the quantum system in contact with the surrounding environment, it is crucial to maintain the coherence by external active manipulation of the target quantum system.

At present, there are two methods to suppress decoherence that are proposed theoretically. One of these is to utilize quantum error correcting code[62, 63]. The other promising and efficient method of preventing decoherence is the so-called bang-bang control by shining repetitive intense laser pulses on the target quantum system[64].

Although the methods mentioned above are proposed to be applied to simple two-level quantum systems (qubits), most quantum systems are composed of many eigenstates (qudits), e. g., molecular internal degrees of freedom. Therefore, the analytical approaches of the error correcting code and the bang-bang control cannot easily be extended to qudits such as molecular modes. If this is the case, one has to resort to other methods for the purpose of decoherence suppression of the realistic molecular systems. One of the advantageous methods will be to OCT and apply it to concrete calculations of realistic multi-level quantum systems in order to control the dissipative quantum dynamics most efficiently.

In fact, OCT for dissipative quantum dynamics has attracted much attention in recent years. This is because it is possible to construct laser pulses that can manipulate quantum dynamics efficiently in the presence of the surrounding environment and because it is difficult to predict by intuition what kind of laser pulses are the most appropriate for achieving the target dissipative quantum dynamics. OCT for the dissipative quantum dynamics has been developed and improved by many researchers. For example, the OCT for dissipative quantum systems was constructed in a fully systematic and rigorous fashion by Cao and coworkers for the first time[65]. However, their theory can only be applied to the weak response regime. Almost at the same time, the OCT in the strong response regime was developed in terms of the Liouville-space density matrix[66]. Ohtsuki and coworkers developed a monotonically convergent algorithm for dissipative quantum systems[67] and applied their theory to the control of wavepacket dynamics under the influence of dissipation[68]. Recently, there have appeared several numerical applications of OCT in realistic dissipative media for a variety of purposes. For example, simulations of molecular quantum computers using the vibrational modes of molecules including dissipation have been performed by Ndong and coworkers[27]. Seideman and coworkers have applied dissipative OCT to manipulate rotational wavepacket dynamics in a dissipative environment[69, 70]. From the experimental viewpoint, dissipative OCT was used for the quantum control of I_2 in the gas phase and in condensed phase solid Kr matrix[71].

Also for the quantum control in the dissipative environment, only FIFP-OCTs have been developed. Dissipative quantum dynamics can be regarded as on of the most time-sensitive processes. The reason is that the decoherence rate Γ governs the decoherence degree versus time. Therefore, FRFP-OCT also has a significant importance for dynamical control of dissipative quantum dynamics. If this is the case for the quantum system under investigation, the equation of motion should be replaced by, e. g., the Liouville-von Neumann equation in the framework of the density matrix representation. Consequently, one of the main purposes here is to generalize FRFP-OCT suitable only for pure states to *mixed state* FRFP-OCT following the general Master equation in both Markov approximation and without any approximations.

3.1 FRFP-OCT in pure state

We assume that the quantum system of our interest is separated from the surrounding environment so that our system can adequately be described by the Schrödinger equation. The objective functional of our problem to be maximized is just given by

$$J = \left| \left\langle \Psi_i(T) \middle| \Phi_f \right\rangle \right|^2 , \tag{13}$$

where $|\Psi_i(t)\rangle$ is time-dependent wavefunction at time t and $|\Psi_i(T)\rangle$ is the time-dependent wavefunction at the target final time $t = T$. On the other hand, $|\Phi_f\rangle$ is the final target wavefunction at time $t = T$. Our purpose is to maximize the objective function, J, at some time T. Note that we *do not fix* T while J should be maximized. This kind of problem has not yet been investigated in control problems in quantum mechanics so far. It should be noticed that the objective functional given by Eq. (13) is different from that of the optimal control theory investigated so far. In the conventional FIFP-OCT, the objective functional is usually given by

$$J = \left|\langle \Psi_i(T) | \Phi_f \rangle\right|^2 - \alpha \int_0^T E(t)^2 dt \,, \tag{14}$$

where $E(t)$ is the external laser fields and α is usually called penalty factor that is added to minimize the strength of the external laser fields. Defining the objective functional as Eq. (14) and adding the constraints that the system obeys, Rabitz and coworkers proposed, e. g., monotonically convergent OCT[52].

Let us now derive the quantum mechanical FRFP-OCT that is necessary, e. g., for entanglement generation as mentioned above. First, we introduce *real* time t and *fictitious*-time τ, which are related by the following equality:

$$t = T(\tau)\tau \,, \tag{15}$$

where τ is a dimensionless parameter that ranges from zero to unity In addition, we have included the implicit dependence of T on dimensionless parameter τ in Eq. (15). The time-dependent equation for $|\Psi_i(t)\rangle$ is given by the conventional *real-time* Schrödinger equation:

$$i\hbar \frac{\partial |\Psi_i(t)\rangle}{\partial t} = \left\{\hat{H} - \vec{\mu}\cdot\vec{E}(t)\right\} |\Psi_i(t)\rangle \,, \tag{16}$$

where $\hat{H}$ is the zero-th order Hamiltonian and $-\vec{\mu}\cdot\vec{E}(t)$ is the laser-molecule interaction. Using the relationship of Eq. (15) for Eq. (16), we obtain

$$i\hbar \frac{\partial |\Psi_i(\tau)\rangle}{\partial \tau} = \left\{\hat{H} - \vec{\mu}\cdot\vec{E}(\tau)\right\} |\Psi_i(\tau)\rangle T(\tau) \,. \tag{17}$$

We may call Eq. (17) as *fictitious-time* Schrödinger equation.

Usually, the objective functional to be maximized or minimized is constrained by some of the factors, e. g., the equation of dynamics that the problem in mind follows. In this case, we can add such constraints into Eq. (17) using Lagrange multipliers and we obtain the new objective functional,

$$\hat{J} = \left|\langle \Psi_i(\tau = 1) | \Phi_f \rangle\right|^2 - 2\,\mathrm{Re}\left[\int_0^1 \langle \Psi_f(\tau)| \left\{\frac{i}{\hbar}\left(\hat{H} - \vec{\mu}\cdot\vec{E}(\tau)\right) + \frac{\partial}{T(\tau)\partial\tau}\right\} |\Psi_i(\tau)\rangle T(\tau) d\tau\right]$$

$$- \int_0^1 \nu_T(\tau) \frac{\partial T(\tau)}{\partial \tau} d\tau \,. \tag{18}$$

Then, we introduce the variational principle for Eq. (18). In order for $\hat{J}$ to be maximized, we can deduce the following equations:

$$i\hbar\frac{\partial\left|\Psi_i(\tau)\right\rangle}{\partial\tau}=\left\{\hat{H}-\vec{\mu}\cdot\vec{E}(\tau)\right\}\left|\Psi_i(\tau)\right\rangle T(\tau)$$

subject to the initial condition

$$\left|\Psi_i(\tau=0)\right\rangle=\left|\Phi_i\right\rangle, \tag{19}$$

where $\left|\Phi_i\right\rangle$ is the initial given state.

$$i\hbar\frac{\partial\left|\Psi_f(\tau)\right\rangle}{\partial\tau}=\left\{\hat{H}-\vec{\mu}\cdot\vec{E}(\tau)\right\}\left|\Psi_f(\tau)\right\rangle T(\tau)$$

subject to the initial condition

$$\left|\Psi_f(\tau=1)\right\rangle=\left|\Phi_f\right\rangle, \tag{20}$$

$$\frac{\partial\nu_T(\tau)}{\partial\tau}=-\frac{2}{\hbar}\mathrm{Im}\left\{\left\langle\Psi_f(\tau)\right|\left[\hat{H}-\vec{\mu}\cdot\vec{E}(\tau)\right]\left|\Psi_i(\tau)\right\rangle\right\}$$

subject to the initial condition

$$\nu_T(\tau=1)=2\,\mathrm{Re}\left\{\left\langle\Psi_i(\tau=1)\middle|\Phi_f\right\rangle\left\langle\Phi_f\middle|\frac{\partial\Psi_i(\tau=1)}{T(\tau=1)\partial\tau}\right\rangle\right\}, \tag{21}$$

When Eqs. (19)~(21) are satisfied, we have

$$\delta\hat{J}=\int_0^1 d\tau g(\tau)\delta E(\tau)+\nu_T(\tau=0)\delta T(\tau=0), \tag{22}$$

where we have defined

$$g(\tau)=-\frac{2}{\hbar}\mathrm{Im}\left\{\left\langle\Psi_f(\tau)\middle|\mu\middle|\Psi_i(\tau)\right\rangle\right\}T(\tau). \tag{23}$$

If the correction of the laser amplitude $E(\tau)$ is represented as $\delta E(\tau)$, we define

$$\delta E(\tau)=\alpha g(\tau). \tag{24}$$

On the other hand, if we defined the correction of $T(\tau)$ as $\delta T(\tau)$, we choose

$$\delta T(\tau)=\beta\nu_T(\tau=0). \tag{25}$$

When Eqs. (24) and (25) are inserted into Eq. (22), we obtain

$$\delta\hat{J}=\int_0^1 d\tau\alpha g(\tau)^2+\beta\nu_T(\tau=0)^2. \tag{26}$$

If both α and β are positive, it is expected that the objective reaches maximum monotonically as is clearly understood from Eq. (26). On the other hand, if both α and β are negative, it is expected that the objective reaches minimum monotonically.
Based on the above equations, we have constructed the following FRFP-OCT in pure state following the Schrödinger equation. In what follows, the superscript (*j*) is used to denote the quantities for the *j*-th iteration.

i. One chooses initial guess external fields $E^{(0)}(\tau)$ and nominal $T^{(0)}$ that is the final time of quantum dynamics. Here and in the following, the superscript (*j*) is used to denote the quantity of the *j*-th iteration. In addition, the trial positive parameters α and β are given because our purpose is to maximize Eq. (13).
ii. The Schrödinger equation, Eq. (19), is propagated forwardly in time from $\tau = 0$ to $\tau = 1$ and the obtained wavefunction $\left|\Psi_i^{(j)}(\tau)\right\rangle$ is stored. At the same time, the objective functional $J^{(j)} = \left|\left\langle \Psi_i^{(j)}(T)\middle|\Phi_f\right\rangle\right|^2$ is calculated.
iii. Equations (20) and (21) are propagated backwardly in time from $\tau = 1$ to $\tau = 0$ and the wavefunction $\left|\Psi_f^{(j)}(\tau)\right\rangle$ is stored. In addition, $\nu_T(\tau = 0)$ is calculated.
iv. Using Eqs. (24) and (25), the laser amplitude $E^{(j)}(\tau)$ and $T^{(j)}$ are updated as follows,

$$E^{(j+1)}(\tau) = E^{(j)}(\tau) + \alpha g(\tau), \tag{27}$$

and

$$T^{(j+1)} = T^{(j)} + \beta \nu_T(\tau = 0). \tag{28}$$

v. One sets the convergence criterion η and if the following criterion

$$\left|J^{(j+1)} - J^{(j)}\right| \le \eta \tag{29}$$

is met, the calculation is terminated.
vi. If the convergence is not sufficient, one updates $E^{(j)}(\tau)$ and $T^{(j)}$ to $E^{(j+1)}(\tau)$ and $T^{(j+1)}$, and loops back to the step (ii).

To show how our theory works concretely by showing calculation results, we have applied the above algorithm to tailoring optimal laser pulses that can create the maximally entangled Bell states between NaCl and NaBr molecules coupled by dipole-dipole interaction. One of the calculation examples is shown in Fig. 2.
In Fig. 2, we show the numerical results for the optimization of the quantum transfer $|0,0\rangle \to \left(|0,0\rangle + |1,1\rangle\right)/\sqrt{2}$ with the nominal $T^{(0)}$ = 300 ps. From panel (a), we can see that the rate of the monotonic convergence of the transition probability is better for FRFP-OCT than that for FIFP-OCT. In addition, the finally obtained transition probability is better for FRFP-OCT. On the other hand, from panel (b), it is seen that the temporal duration of the laser pulse becomes longer with the optimization iteration. This reflects the fact that the longer temporal duration of the laser pulse is more favorable than the shorter one because the nominal $T^{(0)}$ was too short to reach a high transition probability. It is clear from panels (d) and (f), the maximally entangled Bell state cannot be created by both FRFP-OCT and FIFP-

OCT. This is because the tailored laser pulses have a short temporal duration so that it is difficult to reach the maximally entangled state as mentioned above. However, it is clearly seen that FRFP-OCT has attained much higher transition probability than FIFP-OCT has (see panel (f)). The optimal time duration of the laser pulse obtained by FRFP-OCT was 327.95 ps. It is expected that the behaviors shown in these figures are also universal to controls of other physical and chemical phenomena.

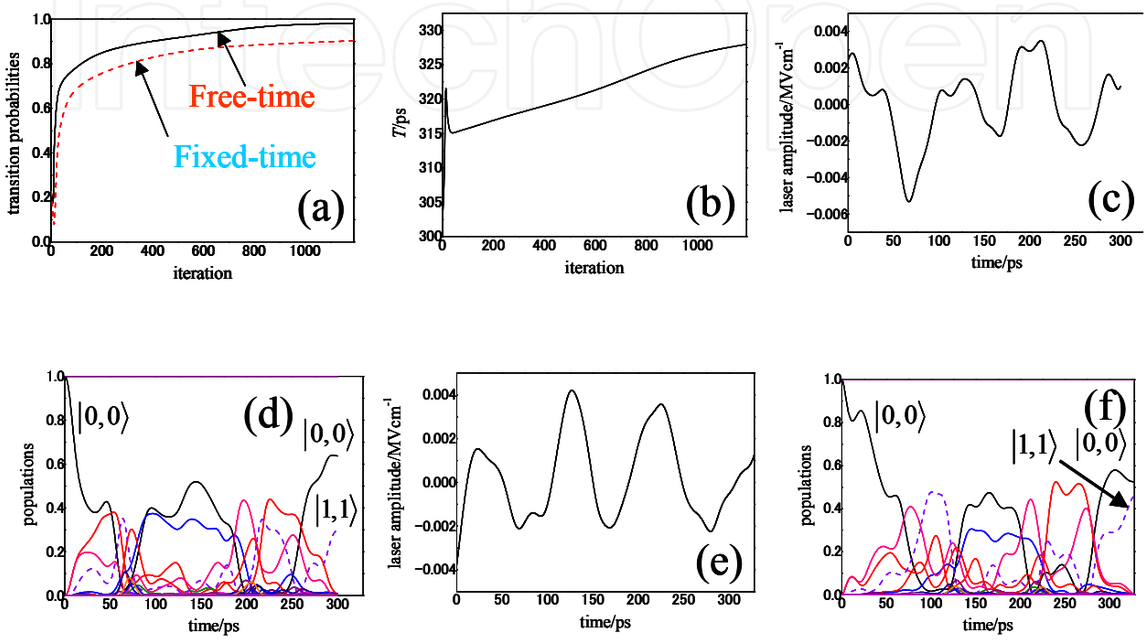

Fig. 2. (a) trasition probability versus iteration number, (b) temporal durationof the optimized laser pulse versus iteration number, (c) optimized laser pulse with α and β being equal to 2×10^{-16} a.u. and 0.0 a.u., respectively, (d) population transfer for panel (c), (e) optimized laser pulse with α and β being equal to $2x10^{-16}$ a.u. and $2x10^{11}$ a.u., respectively, and (f) population transfer for panel (e). The nominal $T^{(0)}$ was set to he 300 ps. The intermolecular distance R is equal to 5.0 nm. In this figure, the target transition $|0,0\rangle \rightarrow (|0,0\rangle + |1,1\rangle)/\sqrt{2}$ was optimized.

From the above numerical results, we can conclude that our FRFP-OCT is much more efficient than the conventional FIFP-OCT because the temporal duration of the laser pulse can also be optimized accurately, which makes OCT more flexible.

3.2 FRFP-OCT in dissipative media

Next, we are interested in the situation where the quantum system of interest is affected by the surrounding environment so that it is necessary to describe the quantum system in the density-matrix representation. In such a case, we start from the assumption that the objective functional to be maximized is simply given by

$$J = \left\langle\left\langle \hat{W} \middle| \hat{\rho}(T) \right\rangle\right\rangle, \tag{30}$$

where $\hat{\rho}(t)$ represents the time-dependent reduced density matrix at time t, $\hat{\rho}(T)$ is the time-dependent reduced density matrix at the target final time $t = T$, and $\hat{W}$ is the objective reduced density matrix. The notation in Eq. (30), $\left\langle\left\langle \hat{B}\middle|\hat{C}\right\rangle\right\rangle$ for arbitrary matrices $\hat{B}$ and $\hat{C}$, is defined by

$$\left\langle\left\langle \hat{B}\middle|\hat{C}\right\rangle\right\rangle = Tr\left(\hat{B}^{\dagger}\hat{C}\right). \tag{31}$$

Equation (31) measures the degree of closeness between the matrices $\hat{B}$ and $\hat{C}$. Then, our purpose is to maximize the objective function, J, at some time T. Note that we *do not fix T* while J should be maximized. It should be noticed that the objective functional given by Eq. (30) is different from that of the conventional FIFP-OCT. In the theory, the objective functional is usually given by[67]

$$J = \left\langle\left\langle \hat{W}\middle|\hat{\rho}(T)\right\rangle\right\rangle - \frac{1}{\hbar A}\int_0^T E(t)^2\,dt\,, \tag{32}$$

where $E(t)$ is the external laser field and the positive constant A is the penalty factor to weigh the significance of the pulse fluence. Because of this difference, our derivation of the OCT in dissipative media is also quite different from theirs.

For the FRFP-OCT, we will again introduced the fictitious time defined by Eq. (15). In real time, the time-dependent equation for the reduced density matrix, $\hat{\rho}(t)$, is expressed as:

$$i\hbar\frac{\partial\hat{\rho}(t)}{\partial t} = \left(\hat{\hat{L}}_0 + \hat{\hat{L}}_{el}(t) - i\hbar\hat{\hat{\Gamma}}\right)\hat{\rho}(t)\,, \tag{33}$$

where

$$\hat{\hat{L}}_0\hat{\rho}(t) = \left[\hat{H}_0\,,\hat{\rho}(t)\right], \qquad \hat{\hat{L}}_{el}(t)\hat{\rho}(t) = \left[\hat{H}_{el}(t),\hat{\rho}(t)\right], \tag{34}$$

and $\hat{\hat{\Gamma}}$ is the damping operator due to the interaction between the system of interest and the surrounding environment. $\hat{H}_0$ is the zeroth-order Hamiltonian and $\hat{H}_{el}(t) = -\vec{\mu}\bullet\vec{E}(t)$ is the laser-molecule interaction with $\vec{\mu}$ being the transition dipole moment. Using the relationship of Eq. (15) for Eq. (33), we obtain the so-called *fictitious time* Master equation,

$$i\hbar\frac{\partial\hat{\rho}(\tau)}{\partial\tau} = \left(\hat{\hat{L}}_0 + \hat{\hat{L}}_{el}(\tau) - i\hbar\hat{\hat{\Gamma}}\right)\hat{\rho}(\tau)T(\tau)\,. \tag{35}$$

When the objective functional to be optimized is constrained by some equations, we should sum up such constraints into Eq. (30) using Lagrange multipliers. Then, we obtain the following new objective function,

$$\begin{aligned}\overline{J} = \left\langle\left\langle \hat{W}\middle|\hat{\rho}(\tau=1)\right\rangle\right\rangle - \int_0^1\left\langle\left\langle \hat{\sigma}(\tau)\right|\left\{\frac{i}{\hbar}\left(\hat{\hat{L}}_0 + \hat{\hat{L}}_{el}(\tau) - i\hbar\hat{\hat{\Gamma}}\right) + \frac{\partial}{T(\tau)\partial\tau}\right\}T(\tau)\left|\hat{\rho}(\tau)\right\rangle\right\rangle d\tau \\ -\int_0^1 \nu_T(\tau)\frac{\partial T(\tau)}{\partial\tau}d\tau\end{aligned} \tag{36}$$

For $\overline{J}$ to be maximized, it is possible to deduce the following equations by applying variational principle to Eq. (36):

$$i\hbar\frac{\partial\hat{\rho}(\tau)}{\partial\tau}=\left(\hat{\hat{L}}_0+\hat{\hat{L}}_{el}(\tau)-i\hbar\hat{\hat{\Gamma}}\right)\hat{\rho}(\tau)T(\tau)$$

subject to the initial condition

$$\hat{\rho}(\tau=0)=\hat{W}_0\,, \tag{37}$$

where $\hat{W}_0$ is the initial fixed reduced density matrix,

$$i\hbar\frac{\partial\hat{\sigma}(\tau)}{\partial\tau}=\left(\hat{\hat{L}}_0+\hat{\hat{L}}_{el}(\tau)-i\hbar\hat{\hat{\Gamma}}\right)^{\dagger}\hat{\sigma}(\tau)T(\tau)$$

subject to the initial condition

$$\hat{\sigma}(\tau=1)=\hat{W}\,, \tag{38}$$

where the superscript, †, denotes Hermitian conjugation,

$$\frac{\partial\nu_T(\tau)}{\partial\tau}=\left\langle\left\langle\hat{\sigma}(\tau)\right|\frac{i}{\hbar}\left(\hat{\hat{L}}_0+\hat{\hat{L}}_{el}(\tau)-i\hbar\hat{\hat{\Gamma}}\right)\left|\hat{\rho}(\tau)\right\rangle\right\rangle$$

subject to the initial condition

$$\nu_T(\tau=1)=\frac{1}{T(\tau=1)}\left\langle\left\langle\hat{W}\right|\partial\hat{\rho}(\tau=1)/\partial\tau\right\rangle\right\rangle\,. \tag{39}$$

When Eqs. (37) - (39) are satisfied, we have

$$\delta\overline{J}=\int_0^1 d\tau g(\tau)\delta E(\tau)+\nu_T(\tau=0)\delta T(\tau=0)\,, \tag{40}$$

where we have defined

$$g(\tau)=\frac{i}{\hbar}\left\langle\left\langle\hat{\sigma}(\tau)\right|\frac{\partial\hat{\hat{L}}_{el}(\tau)}{\partial E(\tau)}\left|\hat{\rho}(\tau)\right\rangle\right\rangle T(\tau)\,. \tag{41}$$

Note that $g(\tau)$ is real. If the correction to the laser amplitude $E(\tau)$ is expressed as $\delta E(\tau)$, we define

$$\delta E(\tau)=\alpha g(\tau)\,. \tag{42}$$

On the other hand, if we define the correction to $T(\tau)$ as $\delta T(\tau)$, we put

$$\delta T(\tau=0)=\beta\nu_T(\tau=0)\,. \tag{43}$$

By inserting Eqs. (42) and (43) into Eq. (40), we obtain

$$\delta\overline{J}=-\int_0^1 d\tau\alpha g(\tau)^2+\beta\nu_T(\tau=0)^2\,. \tag{44}$$

From this equation, it is clear that if α is negative and β is positive, the objective function reaches a maximum monotonically. On the other hand, if α is positive and β is negative, the objective functional reaches minimum monotonically. Here, it should be noted that the units of α and β are Wcm^{-2} and fs^2, respectively.

From the above derivation, we have constructed the following FRFP-OCT in dissipative media following the Master equation. In what follows, the superscript (*j*) is used to denote the quantity for the *j*-th iteration.

i. An initial guess is selected for the external field $E^{(0)}(\tau)$ and initial $T^{(0)}$ that is the final time of the quantum dynamics. In addition, the trial negative and positive parameters, α and β, are given because our purpose is to maximize Eq. (30).

ii. The Master equation of Eq. (37) is propagated forward in time from $\tau = 0$ to $\tau = 1$ and the obtained density matrix $\hat{\rho}^{(j)}(\tau)$ is stored. At the same time, the objective function $J^{(j)} = \left\langle\left\langle \hat{W} \middle| \hat{\rho}^{(j)}(\tau = 1) \right\rangle\right\rangle$ is calculated.

iii. Equations (38) and (39) are propagated backward in time from $\tau = 1$ to $\tau = 0$ and the density matrix $\hat{\sigma}^{(j)}(\tau)$ is stored. At the same time, $\nu_T(\tau = 0)$ is calculated.

iv. The laser amplitude $E^{(j)}(\tau)$ and the temporal duration of the external field $T^{(j)}$ are updated as follows,

$$E^{(j+1)}(\tau) = E^{(j)}(\tau) + \alpha g(\tau), \tag{45}$$

and

$$T^{(j+1)} = T^{(j)} + \beta \nu_T(\tau = 0). \tag{46}$$

v. One sets the convergence criterion η and when the following criterion

$$\left| J^{(j+1)} - J^{(j)} \right| \le \eta \tag{47}$$

is met, the calculation is terminated.

vi. If the convergence criterion of Eq. (47) is not satisfied, $E^{(j)}(\tau)$ and $T^{(j)}$ are updated to $E^{(j+1)}(\tau)$ and $T^{(j+1)}$, respectively, and loop back to step (ii).

To apply the theory and the algorithm developed above and demonstrate numerical tests, we will employ the vibrational degrees of freedom of carbon monoxide adsorbed on the copper (100) surface, CO/Cu(100). In this case, the total Hamiltonian $\hat{H}$ in the absence of the laser fields is expressed as

$$\hat{H} = \hat{H}_0 + \hat{V}, \tag{48}$$

where $\hat{H}_0$ is the kinetic energy operator and $\hat{V}$ is the potential energy operator defined in the next section. When we introduce three coordinates *r*, *Z*, and *X* for CO stretch, CO-surface stretch, and frustrated translation modes, respectively, $\hat{H}_0$ is given by

$$\hat{H}_0 = -\frac{\hbar^2}{2\mu_{CO}}\frac{\partial^2}{\partial r^2} - \frac{\hbar^2}{2m_{CO}}\frac{\partial^2}{\partial Z^2} - \frac{\hbar^2}{2m_{CO}}\frac{\partial^2}{\partial X^2}, \tag{49}$$

where the masses are

$$\mu_{CO} = \frac{m_C m_O}{m_C + m_O} = 6.856 \text{ amu}, \; m_{CO} = m_C + m_O = 27.995 \text{ amu}. \tag{50}$$

The eigenstates and eigenenergies of the Hamiltonian, $\hat{H}$, are calculated from

$$\hat{H}\left|n_r, n_Z, n_X\right\rangle = E_n \left|n_r, n_Z, n_X\right\rangle , \tag{51}$$

where we have used the abbreviation $\left|n\right\rangle \equiv \left|n_r, n_Z, n_X\right\rangle$ and E_n is the eigenenergy of the state $\left|n\right\rangle$. Here, n_r , n_Z , and n_X denote the quanta of vibrational modes, CO stretch, CO-surface stretch, and frustrated translation, respectively.
The Liouville-von Neumann equation in the Markov approximation in the energy representation is explicitly expressed as

$$\frac{d\rho_{nn}(t)}{dt} = -\frac{i}{\hbar} E_z(t) \sum_{i=1}^{N} \left\{ \mu_{ni}\rho_{in}(t) - \rho_{ni}(t)\mu_{in} \right\} + \sum_{i=1}^{N} \left\{ \Gamma_{i\to n}\rho_{ii}(t) - \Gamma_{n\to i}\rho_{nn}(t) \right\} \tag{52}$$

for the diagonal elements (populations) of the reduced density matrix and

$$\frac{d\rho_{mn}(t)}{dt} = -i\omega_{mn}\rho_{mn}(t) - \frac{i}{\hbar} E_z(t) \sum_{i=1}^{N} \left\{ \mu_{mi}\rho_{in}(t) - \rho_{mi}(t)\mu_{in} \right\} - \gamma_{m\to n}\rho_{mn}(t) \tag{53}$$

for the off-diagonal elements (coherences). Here, we have defined the energy gap,

$$\omega_{nm} = \left(E_n - E_m\right) / \hbar . \tag{54}$$

The total dephasing rate is given by

$$\gamma_{mn} = \sum_{i=1}^{N} \left(\Gamma_{m\to i} + \Gamma_{n\to i}\right) / 2 + \gamma^{*}_{m\to n} , \tag{55}$$

where $\gamma^{*}_{m\to n}$ is the pure dephasing rate and $\Gamma_{m\to n}$ is the population transfer rate from the state *m* to the state *n*. The values of these parameters were taken from [78]. For the pure dephasing rate, we have taken into account $\gamma^{*}_{(0,0,0)\to(1,0,0)} \approx \gamma^{*}_{(1,0,0)\to(2,0,0)} \approx \gamma^{*}_{(0,0,0)\to(2,0,0)} / 4$ with values taken from Table IV of [72]. For the same reason as mentioned in [72], the precise values of the pure dephasing rates are of no concern in the present calculations.
To check the mixedness of the reduced density matrix in the Hilbert space of our interest (CO stretch and CO-surface stretch modes), we explicitly define it by

$$\text{mixedness} = 1 - Tr_{frust}\left\{\rho(t)^2\right\} , \tag{56}$$

where Tr_{frust} denotes the trace over the frustrated translation mode that is of no concern.

Note that we can apply our algorithm to other types of Master equations in addition to the Liouville-von Neumann equation mentioned above.

We have investigated the configuration of the CO/Cu(100) system shown in Fig. 3. We have taken into account two layers of copper atoms and in each layer the nearest nine Cu atoms in the same manner as in [73].

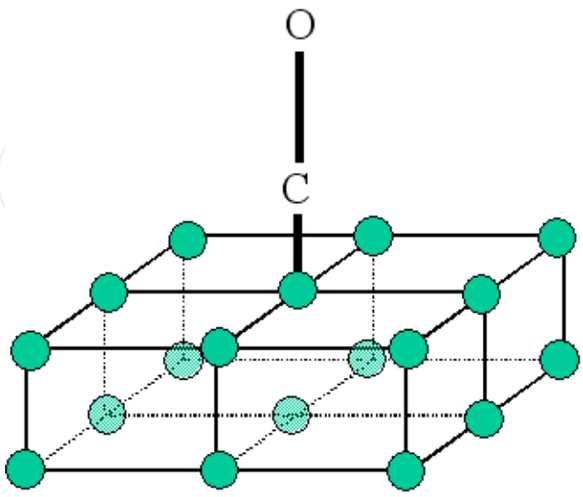

Fig. 3. Schematic of the dissipative CO/Cu(100) system used to apply FRFP-OCT in dissipative media. The Solid circles represent Cu atoms.

The purpose here is two-folds. First, we shall tailor the optimal laser pulses that create maximally entangled Bell state $\left(|0,0,0\rangle+|1,1,0\rangle\right)/\sqrt{2}$ from the separable state $|0,0,0\rangle$. Of course, this is of fundamental importance for quantum computing and quantum information science. Second, we assume that the maximally entangled state, $\left(|0,0,0\rangle+|1,1,0\rangle\right)/\sqrt{2}$, is prepared at t = 0 fs. We shall examine by what kinds of laser pulses this state is maintained in the presence of dissipation. That is, our target transition is $\left(|0,0,0\rangle+|1,1,0\rangle\right)/\sqrt{2}\rightarrow\left(|0,0,0\rangle+|1,1,0\rangle\right)/\sqrt{2}$. This problem seems to be important to study in detail because it may be necessary to maintain some specific entangled sates during other processes in large-scale quantum computers composed of many qubits. Because the effect of decoherence generally seems to be negligible in low temperatures, it may be difficult to show the influence of dissipation on the optimal control. Therefore, we shall mainly present numerical results at high temperatures in the following.

In Fig. 4, we show the case where the initial temporal duration of the laser pulse, $T^{(0)}$, is 1000 fs. The maximum transition probability is attained at T = 996.219 fs, as shown in panel (c). In this case, the incident laser pulse has a shape quite different from that of the other cases. As is clear from panel (a), the laser amplitude from the initial time t = 0 fs to around the time t = 800 fs is quite small (~4 MVcm^{-1}). Therefore, we can hardly observe the population transfer due to the laser pulse. Instead, we can see a significant population transfer from the state $|0,0,0\rangle$ to the state $|0,0,1\rangle$ because of the large population transfer rate, $1/\Gamma_{(0,0,0)\rightarrow(0,0,1)}=3.3$ ps. This transition represents the absorption of the single reservoir quantum by the frustrated translation mode. From the time t = 800 fs to the optimal final time T = 996.219 fs, the amplitude of the optimized laser pulse is quite large (~60 MVcm^{-1}) so that a significant population transfer from the state $|0,0,0\rangle$ to the target state $|1,1,0\rangle$ takes

place and coherence between the states, $|0,0,0\rangle$ and $|1,1,0\rangle$, builds up during this period. These trends are reasonable because if the transition to the target state $|1,1,0\rangle$ occurred much earlier as the result of intense laser pulses, the damping of the population of the state $|1,1,0\rangle$ to other states and the decoherence could be quite significant, which would lead to much larger mixedness and a lower transition probability.

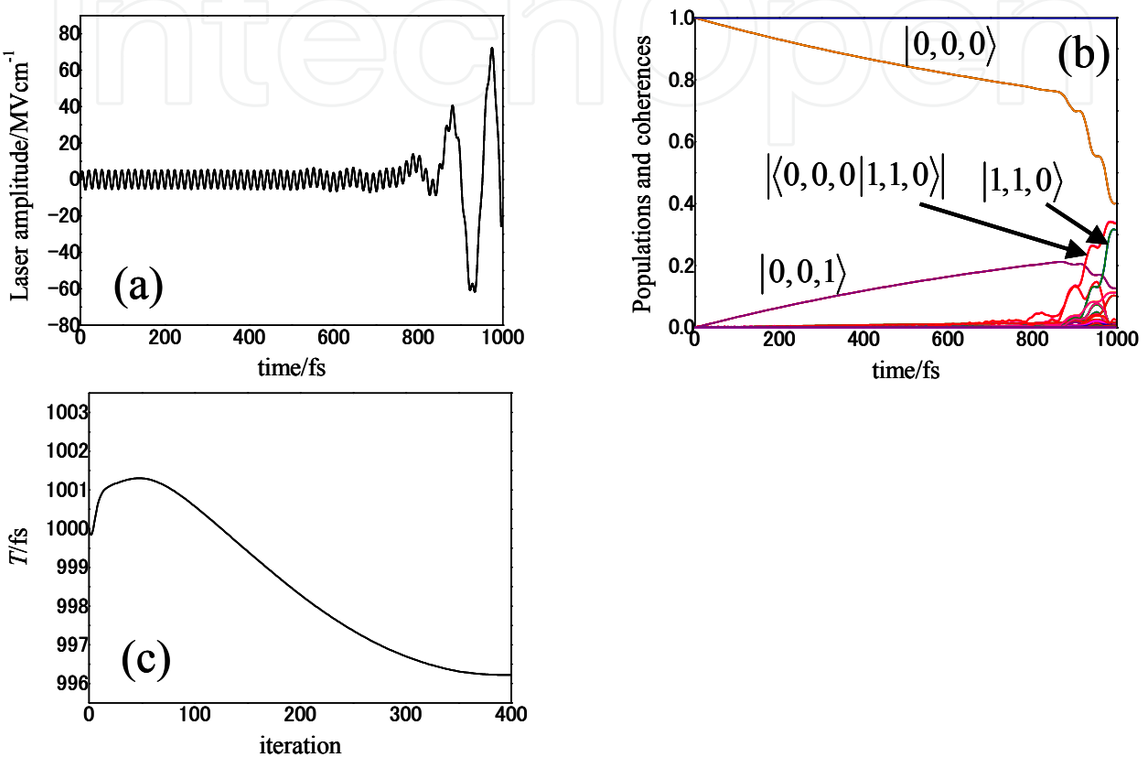

Fig. 4. (a) optimized laser pulse with α and β being equal to -1.755 x10^9 Wcm^{-2} and 5.851 x 10^2 fs^2, respectively, (b) population transfer induced by the optimized laser pulse of panel (a), (c) temporal duration of the optimized laser pulse versus iteration number. The initial $T^{(0)}$ was set to be 1000 fs. The temperature was 300 K. The target transition $|0,0,0\rangle \rightarrow (|0,0,0\rangle + |1,1,0\rangle)/\sqrt{2}$ was optimized.

When the initial temporal duration, $T^{(0)}$, is 1000 fs and the temperature is 300 K, we observe that the temporal duration becomes a little bit longer, T = 1040.56 fs, as can be seen in Fig. 5. The transition probability and the mixedness at the final time are 66.3430% and 0.50711 for the free-time case and are 65.8890% and 0.50515 for the fixed-time case, respectively. In both the free-time and fixed-time cases, the shape of the optimized laser pulses is interesting (here, we do not show the results for the fixed-time case). For the initial half time of total duration, the amplitude of the laser pulse is strong. In the middle of the temporal duration, it becomes weak. After that, the amplitude of the laser pulse becomes stronger with time. This tendency can be explained as follows. Because it is known that the population of the state $|0,0,0\rangle$ can be excited to the state $|0,0,1\rangle$ during the time evolution because of the

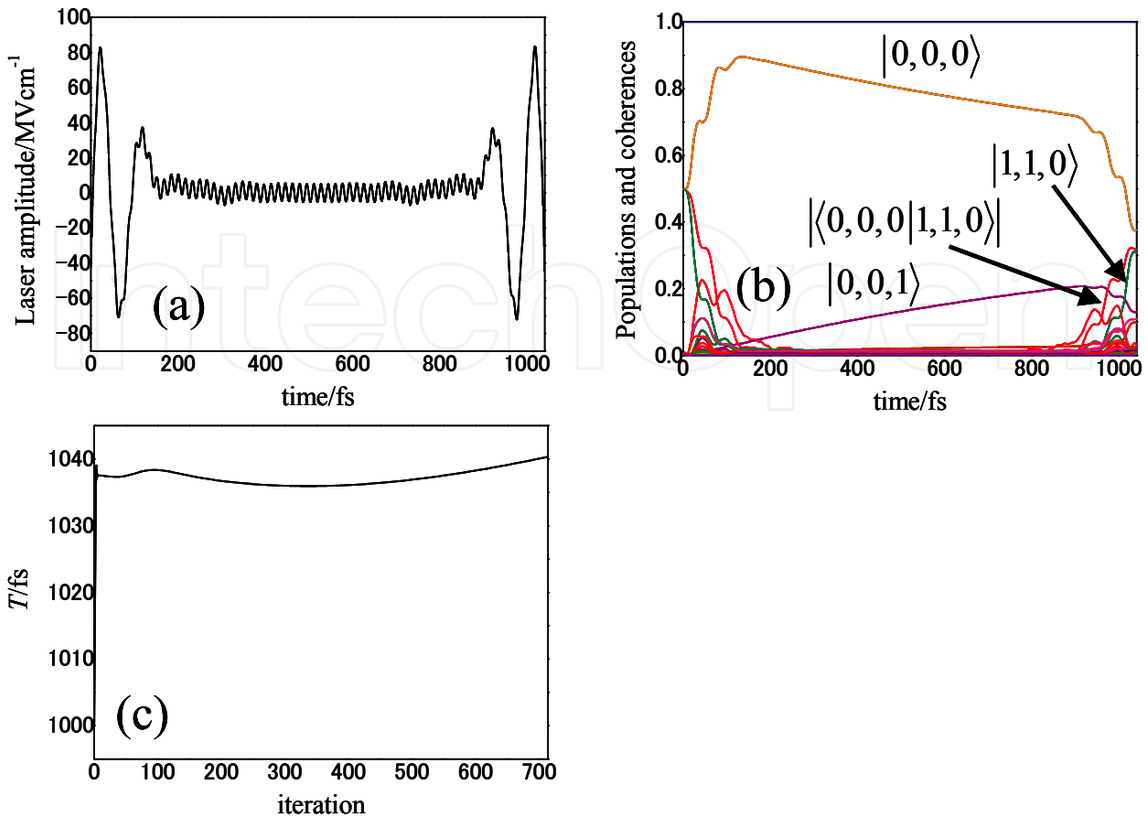

Fig. 5. (a) optimized laser pulse with α and β being equal to -1.755 x10^9 Wcm^{-2} and 5.851 x 10^2 fs^2, respectively, (b) population transfer induced by the optimized laser pulse of panel (a), and (c) temporal duration of the optimized laser pulse versus iteration number. The initial $T^{(0)}$ was set to be 1000 fs. The temperature was 300 K. The target transition $\left(|0,0,0\rangle+|1,1,0\rangle\right)/\sqrt{2} \rightarrow \left(|0,0,0\rangle+|1,1,0\rangle\right)/\sqrt{2}$ was optimized.

dissipative effect as mentioned above, the population of the state $|0,0,0\rangle$ has to increase for the initial half time of total duration using the large intensity of the laser pulse. During this period, almost all the population of the state $|1,1,0\rangle$ contributes to the population increase of the state $|0,0,0\rangle$. For the last half period of the total duration, because of the large intensity of the laser pulse, almost all the population of the state $|0,0,0\rangle$ is excited to the state $|1,1,0\rangle$, as in the cases shown above, and the optimized laser pulse tries to recover the initial maximally entangled state, $\left(|0,0,0\rangle+|1,1,0\rangle\right)/\sqrt{2}$, as much as possible. The reason for the lengthening of the temporal duration compared with the initial guess is that the additional time duration required by the initial recovery of the state $|0,0,0\rangle$ was absent for the target transition $|0,0,0\rangle \rightarrow \left(|0,0,0\rangle+|1,1,0\rangle\right)/\sqrt{2}$ shown in Fig. 4.

Figure 6 shows the case where $T^{(0)}$ is 1000 fs and the temperature is 10 K. Comparing panel (a) with panel (a) of Fig. 5, the pulse shapes are rather similar although the temperatures are quite different. However, because of their small difference, the optimized laser pulse in Fig. 6

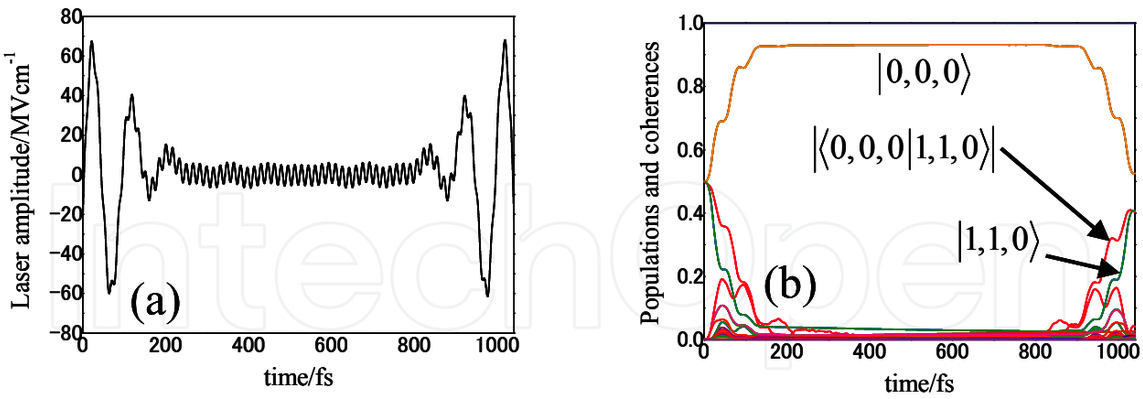

Fig. 6. (a) optimized laser pulse with α and β being equal to -1.755 x10^9 Wcm^{-2} and 2.340 x 10^1 fs^2, respectively, (b) population transfer induced by the optimized laser pulse of panel (a). The initial $T^{(0)}$ was set to be 1000 fs. The temperature was 10 K. The target transition $\left(|0,0,0\rangle+|1,1,0\rangle\right)/\sqrt{2} \rightarrow \left(|0,0,0\rangle+|1,1,0\rangle\right)/\sqrt{2}$ was optimized.

creates the population of the state $|0,0,0\rangle$ as much as possible until around t = 200 fs. Unlike panel (b) of Fig. 5, that of Fig. 6 does not show any significant change of population of the state $|0,0,0\rangle$ during the period when the laser pulse is almost off (from around t = 200 fs to around t = 900 fs). This is also due to the small population transfer rate, $1/\Gamma_{(0,0,0)\rightarrow(0,0,1)} = 85300.0$ ps. Therefore, the transition probability is much larger and the mixedness is much smaller than in the case of Fig. 5. That is, the transition probability and the mixedness at the final time are 86.9429% and 0.22626 for the free-time case and are 86.7598% and 0.23058 for the fixed-time case, respectively. In addition, the optimal temporal duration is also longer than the initial guess: T = 1041.12 fs. The reason is the same as that for Fig. 5.

4. Concluding remarks

In the present chapter, we have reviewed our recent main theoretical and numerical contributions to the development of molecular quantum computing and quantum information science. In particular, we have paved a new way for extending the conventional FIFP-OCT to FRFP-OCT.

Now, quantum computing and quantum information science have become an unshakeable important research topics, ranging among a variety of disciplines. However, some basics of the theoretical aspects have not yet been solved and are still debatable. For instance, the definition of multipartite entanglement degree in pure and mixed states is still discussed in the recently published papers. In addition, scalability and decoherence of quantum states in quantum computers have gradually become obvious to be extremely challenging with the rapid development of experiments and theories. At the same time, the experimental realization of quantum computers based on the theories is also very important in order to extremely outperform the present-day classical computers. Although there are a number of experimental data for physical systems, at present there are few experimental evidences for molecules which chemists are interested in. Therefore, we suspect that there may be a

number of rooms for improvement in molecular quantum computers. We chemists hope that molecular quantum computing will be investigated in more detail from the chemical viewpoint in future. In particular, we expect that our and other's theoretical and numerical results will provide important guides to experimental realization of quantum computers and quantum information processing.

Although we have applied our FRFP-OCT to two specific control problems as shown in Section 3, the theory is so general that it may be possible to apply it to a variety of quantum control problems with and without dissipation in future. An experimental application of FRFP-OCTs developed by us for the first time could be expected in the same manner as closed-loop quantum learning control experiments[74 - 77].

Finally, as for the recent advancement of free-time and fixed end-point *multi-target* optimal control theory, the readers are referred to [78].

5. References

[1] M. A. Nielsen, I. Chuang, *Quantum Computation and Quantum Information*, Cambridge Univ. Press, Cambridge, UK, 2000.
[2] C. H. Bennett, G. Brassard, C. Crepeau, R. Jozsa, A. Peres, and W. K. Wootters, Phys. Rev. Lett. 70, 1895 (1993).
[3] C. Bennett and S. J. Wiesner, Phys. Rev. Lett. 69, 2881 (1992).
[4] M. Brune, F. Schnidt-Kaler, A. Maali, J. Dreyer, E. Hagley, J. Raimond, and S. Haroche, Phys. Rev. Lett. 76, 1800 (1996).
[5] D. L. Moehring, P. Maunz, S. Olmschenk, K. C. Younge, D. N. Matsukevich, L.-M. Duan, and C. Monroe, Nature, 449, 68 (2007).
[6] J. Benhelm, G. Kirchmair, C. F. Roos, and R. Blatt, Nature Phys. 4, 463 (2008).
[7] Friedenauer, H. Schmitz, J. T. Glueckert, D. Porras, and T. Schaetz, Nature Phys. 4, 757 (2008).
[8] G. K. Brennen, C. M. Caves, P. S. Jessen, and I. H. Deutsch, Phys. Rev. Lett. 82, 1060 (1999).
[9] I. L. Chuang, L. M. K. Vandersypen, X. Zhou, D. W. Leung, and S. Lloyd, Nature, 393, 143 (1998).
[10] J. A. Jones and M. Mosca, J. Chem. Phys. 109, 1648 (1998).
[11] J. Clarke and F. K. Wilhelm, Nature, 453, 1031 (2008).
[12] B. E. Kane, Nature, 393, 133 (1998).
[13] A. P. Nizovtsev, S. Ya. Killin, F. Jelezko, T. Gaebal, I. Popa, A. Gruber, J. Wrachtrup, Optics and Spectroscopy, 99, 248 (2004).
[14] P. Neumann, N. Mizouchi, F. Rempp, P. Hemmer, H. Watanabe, S. Yamasaki, V. Jacques, and T. Gaebel, Science, 320, 1326 (2008).
[15] M. Tesch, L. Kurtz, and R. de Vivie-Riedle, Chem. Phys. Lett. 343, 633 (2001).
[16] M. Tesch and R. de Vivie-Riedle, Phys. Rev. Lett. 89, 157901 (2002).
[17] M. Tesch and R. de Vivie-Riedle, J. Chem. Phys. 121, 12158 (2004).
[18] U. Troppmann, C. M. Tesch, and R. de Vivie-Riedle, Chem. Phys. Lett. 378, 273 (2003).
[19] B. M. R. Korff, U. Troppmann, K. L. Kompa, and R. de Vivie-Riedle. J. Chem. Phys. 123, 244509 (2005).
[20] U. Troppmann, C. Gollub, and R. de Vivie-Riedle, New J. Phys. 8, 100 (2006).
[21] C. Gollub and R. de Vivie-Riedle, J. Chem. Phys. 128, 167101 (2008).
[22] Babikov, J. Chem. Phys. 121, 7577 (2004).

[23] M. Zhao and D. Babikov, J. Chem. Phys. 125, 024105 (2006).
[24] M. Zhao and D. Babikov, J. Chem. Phys. 126, 204102 (2007).
[25] D. Babikov and M. Zhao, J. Chem. Phys. 128, 167102 (2008).
[26] T. Cheng and A. Brown, J. Chem. Phys. 124, 034111 (2006).
[27] M. Ndong, D. Lauvergnat, X. Chapuisat, and M. Desouter-Lecomte, J. Chem. Phys. 126, 244505 (2007).
[28] L. Bomble, D. Lauvergnat, F. Remacle, and M. Desouter-Lecomte, J. Chem. Phys. 128, 064110 (2008).
[29] S. Suzuki, K. Mishima, and K. Yamashita, 2005, Chem. Phys. Lett. 410, 358 (2005).
[30] M. Schröder and A. Brown, J. Chem. Phys. 131, 034101 (2009).
[31] See, for example, S. A. Rice and M. Zhao, *Optical Control of Molecular Dynamics*, Wiley-Interscience Publication, John Wiley & Sons, Inc., 2000.
[32] Y. Teranishi, Y. Ohtsuki, K. Hosaka, H. Chiba, H. Katsuki, and K. Ohmori, J. Chem. Phys. 124, 114110 (2006).
[33] A. Shapiro, I. Khavkine, M. Spanner, and M. Yu. Ivanov, Phys. Rev. A 67, 013406 (2003).
[34] M. Tsubouchi and T. Momose, Phys. Rev. A 77, 052326 (2008).
[35] E. Charron, P. Milman, A. Keller, and O. Atabek, Phys. Rev. A 75, 033414 (2007).
[36] K. Mishima and K. Yamashita, Chem. Phys. 361, 106 (2009).
[37] J. Vala, Z. Amitay, B. Zhang, S. R. Leone, and R. Kosloff, Phys. Rev. A 66, 062316 (2002).
[38] M. Tsubouchi and T. Momose, J. Opt. Soc. Am. B 24, 1886 (2007).
[39] Katsuki, H. Chiba, B. Girard, C. Meier, and K. Ohmori, Science 311, 1589 (2006).
[40] K. Ohmori, H. Katsuki, H. Chiba, M. Honda, Y. Hagihara, K. Fujiwara, Y. Sato, and K. Ueda, Phys. Rev. Lett. 96, 093002 (2006).
[41] Katuski, K. Hosaka, H. Chiba, and K. Ohmori, Phys. Rev. A 76, 013403 (2007).
[42] Katsuki, H. Chiba, C. Meier, B. Girard, and K. Ohmori, Phys. Rev. Lett. 102, 103602 (2009).
[43] Ohmori, Annu. Rev. Phys. Chem. 60, 487 (2009).
[44] Mishima, K. Shioya, and K. Yamashita, Chem. Phys. Lett. 442, 58 (2007).
[45] D. Landau, Phys. Z. Sowj. 2, 46 (1932).
[46] C. Zener, Proc. R. Soc. Lond. A 137, 696 (1932).
[47] V. S. Malinovsky and J. L. Krause, Eur. Phys. J. D 14, 147 (2001).
[48] D. P. DiVincenzo, Phys. Rev. A 51, 1015 (1995).
[49] D. Deutsch, Proc. R. Soc. Lond. A 400, 97 (1985).
[50] D. Deutsch and R. Jozsa, Proc. R. Soc. Lond. A 439, 553 (1992).
[51] P. Shor, *Proceedings 35th Annual symposium on Foundations of Computer Science*, 124. (1994).
[52] W. Zhu, J. Botina, and H. Rabitz, J. Chem. Phys. 108, 1953 (1998).
[53] K. Sundermann and R. de Vivie-Riedle, J. Chem. Phys. 110, 1896 (1999).
[54] Y. Ohtsuki, K. Nakagami, Y. Fujimura, W. Zhu, and H. Rabitz, J. Chem. Phys. 114, 8867 (2001).
[55] K. Mishima and K. Yamashita, Chem. Phys. 342, 141 (2007).
[56] K. Mishima and K. Yamashita, Chem. Phys. 352, 281 (2008).
[57] Shapiro and P. Brumer, *Principles of the Quantum Control of Molecular Processes*, Wiley-Interscience, Hoboken, NJ, 2003.
[58] K. Mishima and K. Yamashita, J. Chem. Phys. 130, 034108 (2009).
[59] K. Mishima and K. Yamashita, J. Chem. Phys. 131, 014109 (2009).

[60] W. G. Unruh, Phys. Rev. A 51, 992 (1995).
[61] G. M. Palma, K. –A. Suominen, and A. K. Ekert, Proc. R. Soc. London, Ser. A 452, 567 (1996).
[62] P. W. Shor, Phys. Rev. A 52, R2493 (1995).
[63] A. R. Calderbank and P. W. Shor, Phys. Rev. A 54, 1098 (1996).
[64] L. Viola and S. Lloyd, Phys. Rev. A 58, 2733 (1998).
[65] J. Cao, M. Messina, and K. R. Wilson, J. Chem. Phys. 106, 5239 (1997).
[66] J. Cheng, Z. Shen, and Y. Yan, J. Chem. Phys. 109, 1654 (1998).
[67] Y. Ohtsuki, W. Zhu, and H. Rabitz, J. Chem. Phys. 110, 9825 (1999).
[68] Y. Ohtsuki, K. Nakagami, W. Zhu, and H. Rabitz, Chem. Phys. 287, 197 (2003).
[69] S. Ramakrishna and T. Seideman, J. Chem. Phys. 124, 034101 (2006).
[70] A. Pelzer, S. Ramakrishna, and T. Seideman, J. Chem. Phys. 129, 134301 (2008).
[71] C. J. Bardeen, J. Che, K. R. Wilson, V. V. Yakovlev, V. A. Apkarian, C. C. Martens, R. Zadoyan, B. Kohler, and M. Messina, J. Chem. Phys. 106, 8486 (1997).
[72] S. Beyvers, Y. Ohtsuki, and P. Saalfrank, J. Chem. Phys. 124, 234706 (2006).
[73] C. Cattarius and H.-D. Meyer, J. Chem. Phys. 121, 9283 (2004).
[74] D. Cardoza, C. Trallero-Herrero, F. Langhojer, H. Rabitz, and T. Weinacht, J. Chem. Phys. 122, 124306 (2005).
[75] P. Gross, D. Neuhauser, and H. Rabitz, J. Chem. Phys. 98, 4557 (1993).
[76] RS. Judson and H. Rabitz, Phys. Rev. Lett. 68, 1500 (1992).
[77] R. J. Levis and H. A. Rabitz, J. Phys. Chem. A 106, 6427 (2002).
[78] K. Mishima and K. Yamashita, Chem. Phys. 379, 13 (2011).

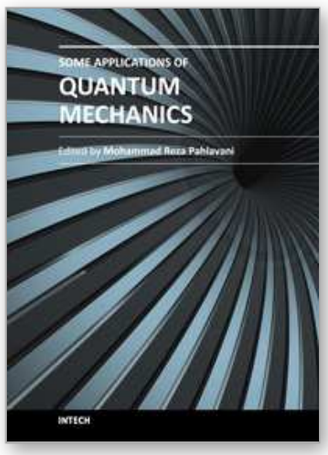

Some Applications of Quantum Mechanics

Edited by Prof. Mohammad Reza Pahlavani

ISBN 978-953-51-0059-1
Hard cover, 424 pages
Publisher InTech
Published online 22, February, 2012
Published in print edition February, 2012

Quantum mechanics, shortly after invention, obtained applications in different area of human knowledge. Perhaps, the most attractive feature of quantum mechanics is its applications in such diverse area as, astrophysics, nuclear physics, atomic and molecular spectroscopy, solid state physics and nanotechnology, crystallography, chemistry, biotechnology, information theory, electronic engineering... This book is the result of an international attempt written by invited authors from over the world to response daily growing needs in this area. We do not believe that this book can cover all area of application of quantum mechanics but wish to be a good reference for graduate students and researchers.

InTech Europe
University Campus STeP Ri
Slavka Krautzeka 83/A
51000 Rijeka, Croatia
Phone: +385 (51) 770 447
Fax: +385 (51) 686 166
www.intechopen.com

InTech China
Unit 405, Office Block, Hotel Equatorial Shanghai
No.65, Yan An Road (West), Shanghai, 200040, China
中国上海市延安西路65号上海国际贵都大饭店办公楼405单元
Phone: +86-21-62489820
Fax: +86-21-62489821

IntechOpen